ORIGINAL ARTICLE

The Impact of Land Use/Land Cover (LULC) Changes on Land Surface Temperature in Sivas City Center and Its Surroundings and Assessment of Urban Heat Island

Can Bülent Karakuş[1]

Abstract

Determination of LULC (land use/land cover) changes in urban planning studies is very important. However, LST (land surface temperature) and UHI (urban heat island) directly associated with LU changes are the parameters that should be considered in similar studies. Therefore, Remote Sensing (RS) and Geographic Information Systems (GIS) are commonly used for obtaining this kind of information. In this study, the relationship between LULC, NDVI (Normalized Difference Vegetation Index) and LST in Sivas city center and its surroundings was studied by using Landsat satellite images from 1989 to 2015 and UHI intensity was also demonstrated. The results clearly show that the urban built-up areas and agricultural lands increased while barren land decreased over the study period. The changes in LST can be monitored depending on the construction materials such as the presence of green areas, the city's unique geographical location and topography. Urban built-up and bare lands have the highest LST and the urban built-up surface temperature showed a fluctuating trend while the rural area temperature showed a tendency to decrease. The urban built-up areas increased, a positive UHI intensity was observed and also an urban heat island formation was determined.

Keywords Land use/land cover · Land surface temperature · Urban heat island · Landsat images · Normalized difference vegetation index · Sivas

1 Introduction

In the globalizing world, more than half of the world's population lives in urban areas. The projected world population in 2050 will cause many changes depending on the size and spatial distribution of the global population (United Nations 2014). The need for natural resources is increasing day by day with the rapid population growth in the world, and it seems that this situation puts an increasing pressure on the natural habitats (FAO 1997). Better introducing and management of the urban environment, given population growth and natural resources, is made possible by urban sustainability (Imhoff et al. 2010). In this regard, LULC changes should be considered as the most basic information in land management

(Chaudhuri and Mishra 2016). These kinds of changes are due to the rapid dissemination that involving large areas rapidly (Rembold et al. 2000), which contributes to LU policy and decision makers in predicting the direction of the human induced environmental changes (Xiao and Weng 2007; Zhang et al. 2013). To fully understand the LU change caused by human activity, LU change information is needed (Omran 2012; Sajikumar and Remya 2015). As stated by Melesse (2004), the current land-use change information is important in environmental monitoring, management and planning (Zhang et al. 2009). Reported studies show that urban growth, particularly the movement of residential and commercial land to rural areas, occur so rapidly (Hegazy and Kaloop 2015); changes occur rapidly; and updated LULC change maps contribute to the monitoring of urban development (Schneider and Woodcock 2008).

LULC changes is known to be the main focus of sustainable development (Lambin et al. 2000) and are very important concepts in natural resource management and monitoring (Sinha et al. 2015). For this reason, monitoring of LU variations utilizing updated data by means of forward-looking

---

Responsible Editor: Lei Bi.

✉ Can Bülent Karakuş
  cbkarakus@gmail.com; bkarakus@cumhuriyet.edu.tr

[1] Faculty of Architecture, Department of City and Regional Planning, Sivas Cumhuriyet University, 58140 Sivas, Turkey

strategies are important for urban planners (Mundia and Aniya 2005). Remote sensing, which is a highly-advanced technique, uses a combination of high resolution images and image processing techniques that reveal the changes in LU in an effective way (Herold et al. 2003; Chaudhuri and Mishra 2016). Remote sensing has been used for LULC mapping and change analysis with the aid of different techniques (Butt et al. 2015; Liu and Yang 2015). It was reported that Landsat satellite images are very convenient for LULC change and also for urban regions analysis (Bagan et al. 2010; Bagan and Yamagata 2012; Mei et al. 2016).

One of the most important indicators of urbanization is the increase of surface temperature with the anthropogenic heat effect and the formation of urban heat island (Kumar et al. 2012). Urban cities are warmer compared to surrounding rural areas (Oke 1973; Chakraborty et al. 2015). Urban heat island (UHI) is known as a problem that occurs as a result of the uncontrolled growth of urban areas (Mirzaei et al. 2012; Yang et al. 2015). The main reason for the formation of urban heat island is warming of the land surface with the effect of material involving the heat due to urban development (Kaya et al. 2012; Hansen 2010). The temperature differences between urban and rural areas are observed due to UHI especially in summer nights (Dhalluin and Bozonnet 2015). Urban heat island affected by the geographical location of a city and the local weather conditions is known as the adverse effect of buildings in urban areas on the climate due to changes in the thermal properties of the urban infrastructure (EPA 2008).

UHI can be expressed generally by air temperature and LST (Li et al. 2014), LST can be easily obtained from remotely-sensed images (Heinl et al. 2015; Feng et al. 2014; Weng 2009). As reported before by Xu et al. (2010), remotely-sensed data are able to demonstrate the relationship between LST and different LULC (Balcik 2014). Landsat TM/ETM+ data have been widely used to perform the analysis of the UHI (Xian and Crane 2006). On the other hand, thermal imagery is very useful to understand UHI taking into account the changes in LULC (Li et al. 2012). The global climate change and increase in the LST arises as a result of rapid urbanization (Streutker 2002; Amanollahi et al. 2016). Therefore, the importance of urbanization on global climate change is greater (Trenberth et al. 2007; Liu et al. 2014; Mathew et al. 2016). The relationship between LULC and LST contributes significantly to determine the effect of LULC change on the LST (Ramachandra and Kumar 2009; Lo and Quattrochi 2003; Deosthali 2000). LULC changes and LST are important components in LU management; and NDVI is a parameter that has a direct influence on UHI analysis (Zhang et al. 2009). Based on the aforementioned relationship between LST and NDVI, LULC change will indirectly affect the LST due to the variation in NDVI among different LULC types (Leong et al. 2015). It can be considered that NDVI and surface temperature depend on land-use changes and on climate change and

global warming (Schultz and Halpert 1993). The average surface temperature of our planet is mainly controlled by albedo and atmospheric greenhouse effect (Varotsos 2002; Efstathiou et al. 2003; Varotsos et al. 2014). Albedo reduction due to snow melting causes more sunlight absorption and increases the surface temperature (Pegau and Paulson 2001). The increase in energy absorption emitted by urban surfaces depends on the reductions in Albedo, and the reduction in albedo contributes to increases in air and surface temperature that characterize UHI (Peng et al. 2012; Trlica et al. 2017).

Many studies have investigated the relationship between LULC and LST using remote-sensing imagery on regional and global climate (Mohan and Kandya 2015; Chen et al. 2017; Zhang et al. 2016; Odindi et al. 2015; Jiang et al. 2015; Shen et al. 2015). The relationship between LULC and LST is very important in land management and global climate change studies. This study performed based on remote sensing techniques, reveals the relationships between LULC, LST and NDVI. The study carried out by Karakus et al. (2014) emphasized the importance of RS and GIS techniques in determining changes in LU and, in particular, how this information may be utilized in order to understand changes in LULC using aerial photographs for the years between 1973 and 2005 and Landsat TM/ETM+ satellite images for the years between 1987 and 2002 for the city of Sivas and its environment. The present study aimed to determine the effects of LU change on LST by examining LULC changes and LST distributions and UHI intensity for the Sivas city center and its surroundings years from 1989 to 2015 using Landsat 4 TM/Landsat 7 ETM+/Landsat 8 OLI images.

2 Materials and Methods

2.1 Study Area

Sivas is located in the upper parts of the Kızılırmak River within the central Anatolian region. In Turkey, the province of Sivas is ranked second in terms of surface area (28,488 km^2) after the province of Konya, and is located between 36° and 39°E longitudes and 38° and 41°N latitudes. This study was carried out in the vicinity of the city center of Sivas at 319000–339000–4,389,000-4,415,000 UTM coordinates (Fig. 1). The study area covers the city center of Sivas and its immediate surroundings and covers an area of approximately 206 km^2. A large part of the study area is located in the height class between 1250 and 1300 m where Sivas city center is located. A large part of Sivas city center and its immediate surroundings is located between 0 and 2% and 2–6% slope group interval. The vast majority of the study area consists of conglomerate-sandstone-mudstone, gypsum and alluvial deposits, which are not suitable for settlement areas (GDMRE 2005). Considering the city center of Sivas; the city is located

Fig. 1 Location of study area: **a**) Sivas province in Turkey **b**) Study area in Sivas province
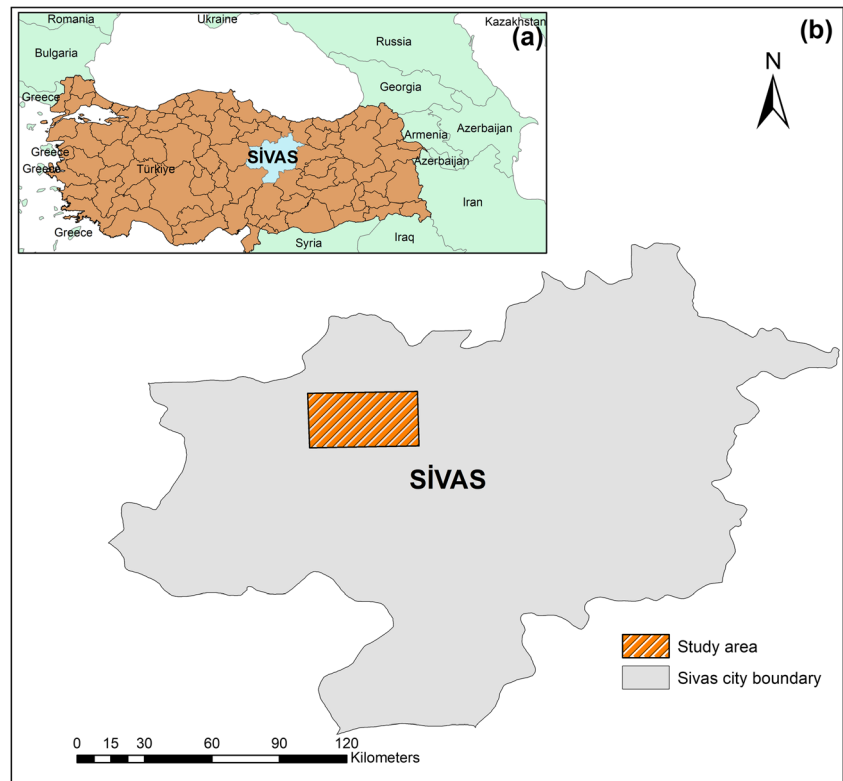
within the alluvial unit which is unsuitable for basic conditions and settlement conditions (GDMRE 1997). Much of the research area is occurs from III., IV. and VII. class lands. The most suitable areas (I. class lands) for agriculture are mostly concentrated along the Kızılırmak river. The unsuitable areas (VIII. class lands) for agriculture are located in the southern part of the study area. The Kızılırmak river passing through the middle of the study area constitutes the most important surface water source of Sivas city and its immediate vicinity (GCM 2005).

It is widely known that Sivas is the coldest city of the central Anatolian region; its temperature may reach 40 °C in summer and can drop to −33 °C in winter. The mean annual precipitation is 420 mm, for four seasons, comprising precipitation of 22% in autumn, 36% in spring, 32% in winter, and 10% in summer. When it comes to plant cover, steppe is the main vegetation of Sivas city and its surroundings (Sivas Governorship 2006). Approximately 50% of the city of Sivas is suitable for agriculture. The population of the city of Sivas began to increase significantly in the late 1930s, especially when state investments began, and as a result, the level of employment increased (Mahiroğulları 2003). According to the 1990 census the population of Sivas city center was 221.512, according to the 2000 census the population of Sivas city center was 251.776, according to the 2015 census the population of Sivas city center was 356.884 (TUIK 2015). When the time interval covering the working period is considered, because of the migration due to economic and social problems, the population greatly increased in the Sivas city center.

2.2 Data Description and Pre-Processing

Landsat-4 TM (acquired on August 27, 1989), Landsat-7 ETM+ (acquired on August 07, 1999) and Landsat-8 OLI (acquired on August 11, 2015) were used in order to determine LULC changes, retrieval of LST, and detect the changes in the UHI in the study area. All image bands 1–5 and 7 have a spatial resolution of 30 m, and the thermal infrared band has a spatial resolution of 60 m for Landsat-4 TM and Landsat-7 ETM+ images and 100 m for Landsat-8 OLI image (Table 1). All Landsat images were provided by the U.S. Geological Survey (USGS). Landsat data are frequently used for land-use and land-cover change analyses (Yuan et al. 2005; Bagan et al. 2010) and are useful for deriving the surface temperature (Kumar et al. 2012). All of the images were clear and nearly free of clouds (total cloud cover less than 10%)with high resolution.

Ancillary data (below) used in this study served as the reference data to determine the LULC variation, aided by the use of satellite images:

a) digitized topographic maps at the scale of 1/25.000 provided by General Command of Mapping of Turkey (GCM)
b) aerial photographs at the scale 1/5.000 from the year 2005 provided by General Command of Mapping of Turkey (HGK)
c) high spatial resolution remote sensing data such as IKONOS (acquired on 2002) provided by Sivas Provincial Directorate of Agriculture (Turkey)

Table 1 Landsat images used in this study

Satellite/Sensor	Acquisition date (YY/MM/DD)	Path/row	Spatial resolution of spectral bands (m)	Spatial resolution of TIR band (m)
Landsat-4 TM (LT4)	1989 − 08-27	174/032	30	60
Landsat-7 ETM+ (LE7)	1999 − 08 − 07	174/032	30	60
Landsat-8 OLI (LC8)	2015 − 08-11	174/032	30	100

d) LU maps obtained from relevant institutions and organizations for the study area

e) point reference data obtained by GPS during field work

All of the images and data were converted in the same coordinate system (UTM/WGS84) to analyze the changes on LULC, LST and NDVI in the study area. All Landsat images were geometrically rectified to a common map reference system (UTM map projection Zone 37 North, WGS84 geodetic datum) based on the IKONOS image and 1/25.000 scale digitized topographic maps. Then all the images (using all bands) were resampled to 30 m using the nearest neighbor method (Xiao and Weng 2007). The RMSE of rectification was less than 0.5. In this study, ERDAS 9.1 was used to determine the LULC variations and for the image processing; and ArcGIS 10.1 was used for the spatial analyses. Furthermore, field type hand-held GPS were also used to identify ground control points.

2.3 Image Processing and Classification

Multi-band satellite images of 1989, 1999 and 2015 were obtained by using all bands of each image and with the help of the ERDAS 9.1 software. A study area covering approximately 206.7 km^2 was extracted as a subset from the Landsat OLI images dated 2015, Landsat ETM+ whole-frame images dated 1999, and Landsat TM images dated 1989, covering an area of 185 km × 185 km. Then false color images produced by assembling bands 5, 4, and 3 of the Landsat TM/ETM+/OLI for visual interpretation in order to correct classification. Visual interpretation can give an idea concerning land cover variation over a particular time period (Shalaby and Tateishi 2007). The goal of image enhancement is to simplify the image interpretability (Karakus et al. 2014).

Remote Sensing (RS) has been used to classify and map the land cover and LU changes using Landsat images in the classification of different landscape components (Ozesmi and Bauer 2002). In this study, Anderson Land Cover Classification System was used. It was originally introduced by Anderson et al. (1976). The LU and LC classification system presented by Anderson et al. (1976) includes only the more generalized first and second levels. "Level 1" includes urban or built-up land, agricultural land, rangeland, forest land, water, wetland, barren land, tundra and perennial snow or ice. To determine variations in LULC and determine the effects of LU changes on LST five LULC classes were identified in this study (Table 2); agriculture, vegetation, urban/built up, water and bare land.

Subsequently, supervised classification was carried out using aerial photographs (inclose dates), ancillary reference data (topographic maps, zoning sheets, etc.), and data gathered in the field. A supervised classification process involving five land classes has been applied with the help of the Maximum Likelihood Algorithm, using all the spectral bands except the 6th spectrum (band), which has thermal characteristics parameters (Karakus et al. 2014). For each image, 100 training sites were selected in order to all spectral range have greater accuracy (Li et al. 2012). Because urban areas with bare land (particularly inclined areas covered with limestone and rocky areas) had similar spectral characteristics, it was difficult to separate these classes in the classification step. The classified images (Fig. 2) were exported to the ArcGIS 10.1 for map preparation.

2.4 Accuracy Assessment

The accuracy evaluation can be done by comparing a reference data with a data obtained with the help of remote sensing (GEOG 2016). In order to perform the accuracy assessment properly, according to Lu and Weng (2007), the number of training samples and their representativeness is important for image classification and the ground data should be collected at a time close to the historical image (Wondrade et al. 2014). To increase classification accuracy of all classified images, ancillary data including digitized topographic maps at the scale of 1/25.000, aerial photographs at the scale 1/5.000 from the year 2005, IKONOS satellite image from the year 2002, point reference data obtained by GPS, Google Earth observations, visual interpretation and our knowledge of the area were used as reference data (Zhang et al. 2013; Li et al. 2012). Reference data were developed for accuracy assessment (Yuan et al. 2005). The reference points formed by a stratified random sampling method was used for accuracy assessment (Xiao and Weng 2007; Wondrade et al. 2014). According to Ji and Niu (2014), confusion matrix computes the

Table 2 Description of LULC classes of in this study area

Land cover (LU/LC) classes	Description
Agriculture	Mechanized and small holder's farms are components of cropland.
Vegetation	Natural forest lined with trees, small grasses are the predominant natural vegetations
Urban/built up	All residential, commercial, and industrial areas; villages; settlements; transportation infrastructure
Water	All areas of open water, including lakes, rivers, and ponds
Bare land	Land without vegetation cover, mainly including exposed soil, sandy and bare rock area

accuracy of each LULC maps (Ghebrezgabher et al. 2016). To calculate producer's accuracy, user's accuracy, and Kappa statistics using reference points, classification results were compared with reference data (Churches et al. 2014). Subsequently, classification results were associated with the reference data for accuracy assessment analysis.

2.5 Retrieval of Brightness Temperature from the Landsat 4 TM/Landsat 7 ETM+/Landsat 8 OLI Images

LST obtained from satellite remotely-sensed thermal infrared (TIR) imagery has an important role in emphasizing the importance of urbanization (Fu and Weng 2016). Thermal band
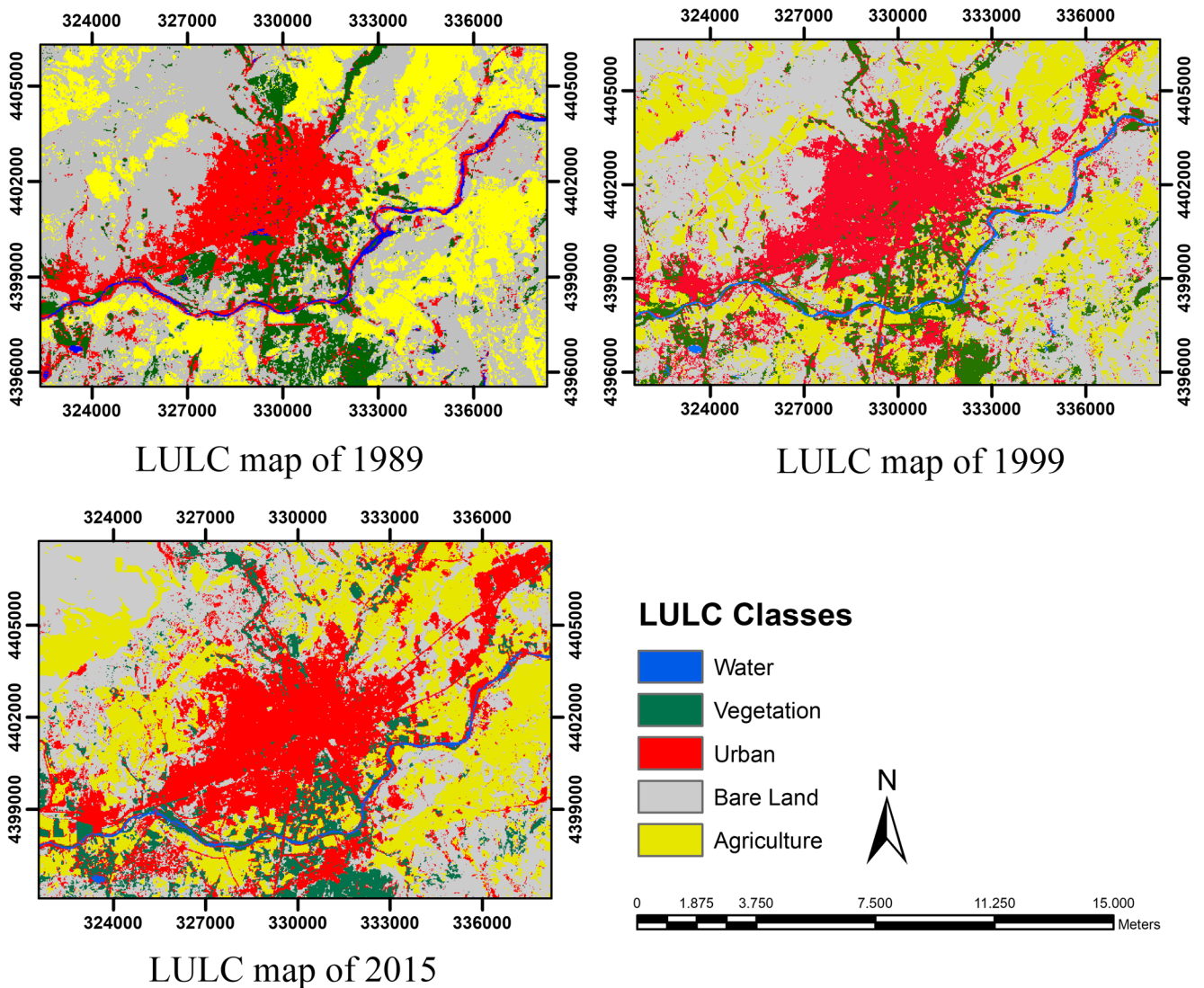

LULC map of 1989

LULC map of 1999

LULC map of 2015

LULC Classes
- Water
- Vegetation
- Urban
- Bare Land
- Agriculture

Fig. 2 Spatial distribution of land use/land cover (LULC) within study area

of Landsat satellite images were used in order to reveal the surface temperature spatial distribution (Ding and Xu 2008) and the impact of LULC on the LST within the study area. The procedure was applied about the LST computation described by Malaret et al. (1985) and Guo et al. (2016). Surface temperature was detected to calculate brightness temperature from thermal band of Landsat satellite images taking into account the minimum and maximum numerical values of each image (Yuksel 2008).

The temperature data can be obtained using the digital images in the thermal band (DN 0–255) of Landsat TM / ETM + / OLI images. Digital numbers (DN) on heat bands (band6, band10) is converted to the Kelvin temperature in two steps. First, the digital number (DN) values of the Landsat images thermal infrared band was converted into spectral radiance using the following equation (Landsat Project Science Office 2002, 2016; Sekertekin et al. 2016):

$$L_\lambda = M_L{}^* Qcal + A_L \qquad (1)$$

$$L_\lambda = \frac{Lmax_\lambda - Lmin_\lambda}{(QCal_{max} - QCal_{min})} \times (QCal_{max} - QCal_{min}) + Lmin_\lambda \qquad (2)$$

where;

L_λ is spectral radiance $W/(m^2 \, sr \, \mu m)$, M_L is radiance multiplicative scaling factor for the thermal bands, cal in Qcal is calibrated standard product, A_L is radiance additive scaling factor for the bands, Qcal is pixel value in DN (digital number), $Qcal_{max} = 255$ ($Qcal_{max}$ is the maximum number of each band), $Qcal_{min} = 1$ ($Qcal_{min}$ is the minimum number of each band), and Lmax and Lmin are spectral radiance for thermal bands at DN 255 and 1, respectively ($W/m^2 \, ster \, \mu m$) (Kumar and Shekhar 2015).

Second TIRS data can also be converted from spectral radiance (as described above) to brightness temperature, which is the effective temperature viewed by the satellite under an assumption of unity emissivity. The conversion formula is as follows (Landsat Project Science Office 2016; Kumar and Shekhar 2015).

$$T = \frac{K_2}{\ln\left[\left(\frac{K_1}{L_\lambda}\right) + 1\right]} \qquad (3)$$

where;

T is brightness temperature in Kelvin, K_1 and K_2 are thermal conversion constant for the band. For Landsat4 TM, $K_1 = 607.76 \, mW/cm^2/sr/\mu m$ and $K_2 = 1260.56$ Kelvin; for Landsat7 ETM+, $K_1 = 666.09 \, mW/cm^2/sr/\mu m$ and $K_2 = 1282.71$ Kelvin; for Landsat8 OLI, $K_1 = 774.89 \, mW/cm^2/sr/\mu m$ and $K_2 = 1321.08$ Kelvin.

2.6 NDVI (Normalized Difference Vegetation Index)

NDVI is a measure of relative greenness (Raynolds et al. 2008) and the NDVI can be used as a general indicator of vegetation cover (Bakr et al. 2010; Wardlow et al. 2006). NDVI is also useful to determine the production of green vegetation as well as detect vegetation changes (Gandhi et al. 2015). NDVI is described as the difference between the near infrared (NIR) and red bands and NDVI values varying between −1 and + 1 values. Non-vegetated surfaces were shown with negative values (Silleos et al. 2006). Higher NDVI values typically indicate areas with dense vegetation (Yuan and Bauer 2007). NDVI was calculated from the red and near infrared bands (Johansen and Tømmervik 2014):

$$NDVI = (NIR - RED)/(NIR + RED) \qquad (4)$$

where; NIR represents the Near Infrared band 4 (0.76–0.90 μm) of Landsat 4 and 7 and RED the corresponding band 3 (0.63–0.69 μm). NIR represents the Near Infrared band 5 (0.85–0.87 μm) of Landsat 8 and RED the corresponding band 4 (0.63–0.67 μm) (Landsat Project Science Office 2016). According to Carlson and Ripley (1997), NDVI values lower than 0.2 represent sparsely vegetated or non-vegetated areas.

2.7 Urban Heat Island Intensity

Urban heat island is the difference in temperature between cities and their surrounding rural zones (Alonso et al. 2007). The meteorological and urbanization factors cause the formation of UHI effects with the increase in urban temperatures due to electricity demand in an urban area (Shahmohamadi et al. 2010). The intensity of urban heat island was defined as the difference between average temperature of UHI area and that of rural area (Ma et al. 2010; Effat et al. 2014; Lee et al. 2012). The TM data was used to perform the UHI detection especially in thermal infrared band (Du et al. 2009).

$$UHI \ intensity \ (^oC) = T_u - Tr$$
$$LST > \mu + 0.5 \times \delta \ referred \ to \ UHI \ area \qquad (5)$$
$$0 < LST \leq \mu + 0.5 \times \delta \ denoted \ non{-}UHI \ or \ rural \ area$$

where; T_u is the urban temperature, and T_r, the rural (surrounding) temperature, μ and δ are the mean and standard deviation of temperatures in study area, respectively.

A positive value indicates the existence of an urban heat island, i.e. the urban temperature is higher than rural. A negative UHI intensity means that the urban temperature is lower than rural temperature and so indicates an urban cool island. The temperatures used in Eq. (5) can be air temperatures, radiant temperatures or surface temperatures. The UHI effect

is commonly quoted based on air temperature with the radiant and surface temperature UHI effects being specifically identified, e.g. UHI (radiant) effect or UHI (surface temperature) effect (Cheung 2011). In hot season, for example in summer, water bodies in urban areas such as ponds, canals and rivers may also have a cooling effect on the surrounding urban area. The cooling effect is caused by evaporation and by heat absorption (Hove et al. 2011).

3 Results and Discussion

3.1 LULC Changes between 1989 and 2015

LULC variations have been determined as five LU categories with corresponding definitions (Table 2). Fig. 2 show the changes in LU/LC during nearly 25-year period. When areal distribution values (Table 3) for LULC for the year 1989, 1999 and 2015 are examined, it is observed that urban built-up area increased rapidly. The urban built-up area increased from 13.37% of the study area in 1989 to 18.08% in 1999 and to 25.72% in 2015. However, bare land decreased from 50.13% of the study area in 1989 to 45.98% in 1999 and to 34.48% in 2015. The area of agricultural land increased rapidly from 26.10% in 1999 to 28.95% in 2015 while the area of agricultural land decreased from 26.47% in 1989 to 26.10% in 1999. During the specified time period, the development of the agricultural areas was observed in the areas outside the Kızılırmak river, and these areas are outside the first class agricultural areas. Population has increased due to the increase in migration from villages to villages and accordingly, the development of agricultural land outside of the first class sites has been determined in these areas. The vegetated area increased from 8.86% in 1999 to 10.03% in 2015 while vegetated area decreased from 9.03% in 1989 to 8.86% in 1999. The main reason of this increase is the improvements made in afforestation around Sivas city center by relevant institutions and organizations. The area of water was 1.00% in 1989,

0.97% in 1999 and 0.82% in 2015. When a general assessment is made for land-use changes over the period 1989–2015, it is observed that urban built-up area (mainly organized industrial zones) was constructed on agricultural land in the north-eastern part of the study area. The development of the residential area was monitored toward the Kızılırmak River which is located on the south of the selected study area. It appears that the most dominant terrain types are agricultural land and bare land in the study area. The increase in urban built-up area and agricultural land is 12.35% and 2.48%, respectively; while a decrease of 15.65% was observed in the bare land between 1989 and 2015. These results have also shown that a majority of bare land (approximately 12.35%) have been converted into urban built-up area. All of the results clearly show that urban built-up have had many changes. The transition to city residential settlements from village, which can be seen for many years in Sivas, was supported in agricultural and residential areas.

Accuracy assessment is an important parameter for urban growth and LST (Wang et al. 2016). The map accuracy procedure defined originally by Congalton (1991) was applied for making the classification accuracy assessment (Saadat et al. 2011). Accuracy assessment analysis of the classification results was performed using Erdas 9.1 at specified time intervals. For this purpose, confusion matrices were obtained to confirm accuracy of the LULC maps (Table 4). Field reference points collected by using a hand-held GPS and ancillary data (aerial photo, IKONOS image) for use in accuracy assessment. A set of 551, 512, and 526 are field reference points for 1989, 1999, and 2015, respectively. It was determined that overall accuracy for the 1989, 1999, and 2015 LULC maps were 84.39%, 90.43%, and 94.11%, respectively. The Kappa coefficient of LULC maps were 0.79, 0.87, and 0.92, respectively. Some LU types (vegetation and water in 1999 and water in 2015) showed 100% producer's accuracy (Table 4). If kappa values are greater than 0.75 and/or 0.80, the classification and reference data are compatible (Wondrade et al. 2014). According to Anderson et al. (1976), minimum

Table 3 Changes in land use/cover obtained Landsat TM/ETM+/OLI images

Land use/ cover (LC) classes	1989		1999		2015		Changes (%) in LULC for 1989–1999	Changes (%) in LULC for 1999–2015	Changes (%) in LULC for 1989–2015
	Area of LULC		Area of LULC		Area of LULC				
	km²	%	km²	%	km²	%			
Agriculture	54.72	26.47	53.94	26.10	59.83	28.95	−0,37	2,85	2,48
Vegetation	18.66	9.03	18.32	8.86	20.73	10.03	-0,17	1,17	1
Urban/built up	27.63	13.37	37.38	18.08	53.17	25.72	4,71	7,64	12,35
Water	2.07	1.00	2.01	0.97	1.69	0.82	-0,03	-0,15	-0,18
Bare land	103.62	50.13	95.05	45.98	71.28	34.48	−4,15	−11,5	−15,65
Total	206.7	100	206.7	100	206.7	100	0	0	0

Table 4 Confusion matrices for the classifications results

1989	Land cover classes	Reference data					Row Total	UA (%)
		Agriculture	Vegetation	Urban/built-up	Water	Bareland		
Classified data	Agriculture	87	2	0	0	18	107	81.31
	Vegetation	3	72	0	0	4	79	91.14
	Urban/built-up	0	0	121	1	20	142	85.21
	Water	0	0	1	45	3	49	91.84
	Bareland	21	0	13	0	140	174	80.46
	Column Total	111	74	135	46	185	551	
	PA (%)	78.38	97.30	89.63	97.83	75.68		
	OA (%)	84.39						
	Kappa	0.79						
1999	Land cover classes	Reference data					Row Total	UA (%)
		Agriculture	Vegetation	Urban/built-up	Water	Bareland		
Classified data	Agriculture	107	0	0	0	16	123	86.99
	Vegetation	0	75	0	0	2	77	97.40
	Urban/built-up	2	0	121	0	5	128	94.53
	Water	0	0	0	51	0	51	100.00
	Bareland	15	0	9	0	109	133	81.95
	Column Total	124	75	130	51	132	512	
	PA (%)	86.29	100.00	93.08	100.00	82.58		
	OA (%)	90.43						
	Kappa	0.87						
2015	Land cover classes	Reference data					Row Total	UA (%)
		Agriculture	Vegetation	Urban/built-up	Water	Bareland		
Classified data	Agriculture	137	0	3	0	10	150	91.33
	Vegetation	0	74	0	0	0	74	100.00
	Urban/built-up	2	2	138	0	9	151	91.39
	Water	0	0	0	50	0	50	100.00
	Bareland	0	0	5	0	96	101	95.05
	Column Total	139	76	146	50	115	526	
	PA (%)	98.56	97.37	94.52	100	83.48		
	OA (%)	94.11						
	Kappa	0.92						

requirement value is 85% for accuracy level by using Landsat satellite images in LULC mapping as suggested USGS (Bakr et al. 2010). It is clearly observed that the accuracy evaluation results obtained from our study is compatible with the values recommended in the literature.

3.2 Relationship between LULC and NDVI

NDVI analysis was performed to confirm LU changes as determined from satellite images and to determine the green areas in the study area using Erdas 9.1. Figure 3 shows spatial distribution of NDVI values within study area. NDVI values are in the range of −0.55 to 0.71, −0.56 to 0.68 and − 0.31 to 0.62 in 1989, 1999 and, 2015, respectively. The average NDVI values were 0.06, 0.08 and 0.15 for 1989, 1999 and

2015, respectively and the average NDVI value increased within the study period. The most important reason of this increase is the enrichment of the green areas especially in and around the Sivas city center according to our own observations. Forest land located in the north of the study area had the highest NDVI values (Xiao and Weng 2007), which were 0.51, 0.44 and 0.60 in 1989, 1999 and 2015, respectively and had the average NDVI as 0.34, 0.29 and 0.41 in 1989, 1999 and 2015, respectively. Fig. 5a show NDVI values associated with different LULC. The higher NDVI values were found over the dense vegetation areas (weighted forest). The lowest NDVI values were observed in urban city (Effat and Hassan 2014), agriculture land and water body for the study area (Fig. 5a). Bare land had the second highest average NDVI values over the study period.
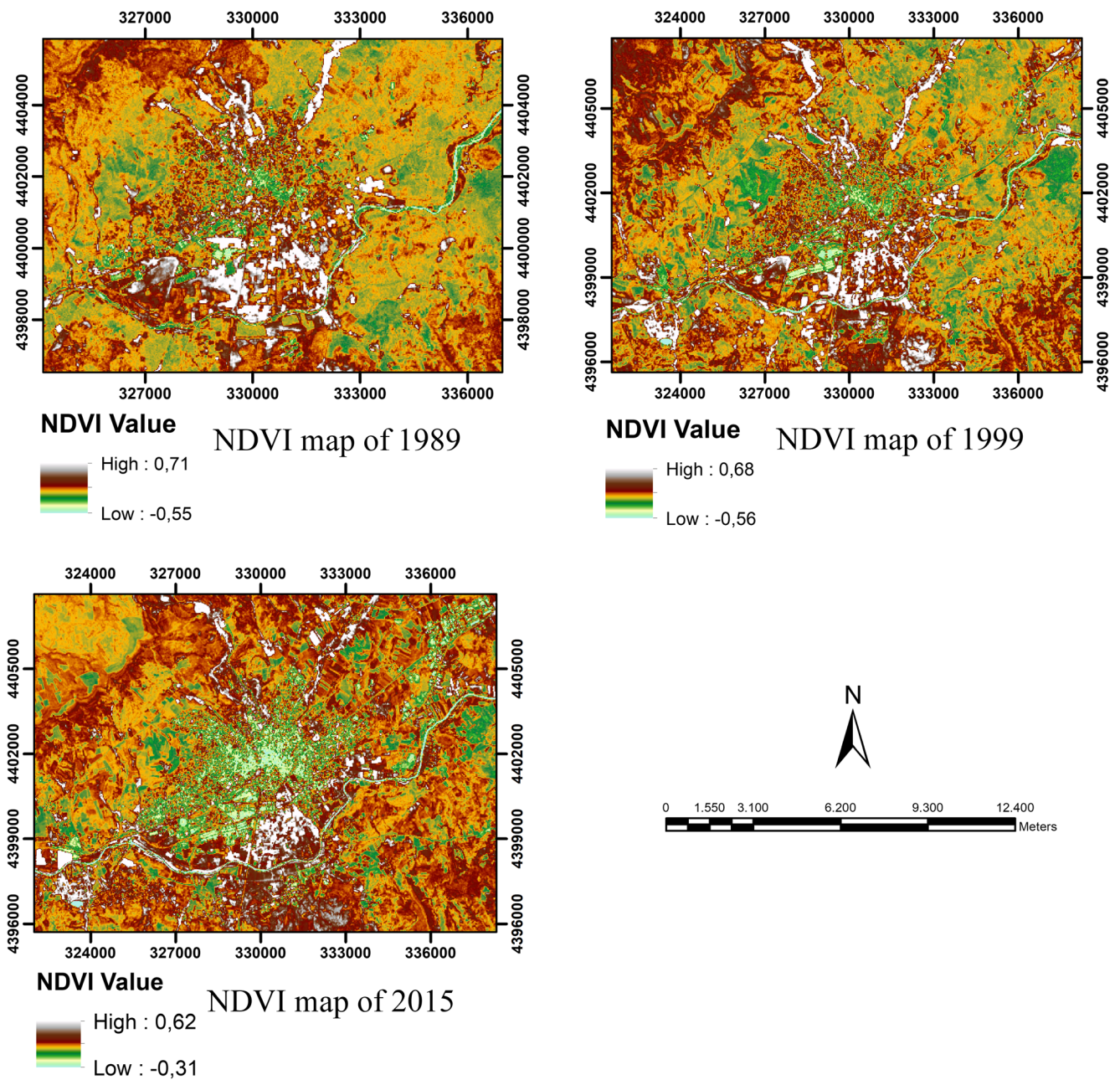
Fig. 3 Spatial distribution of NDVI within study area

NDVI mean values obtained for 1989, 1999 and 2015, respectively in this study are compatible with NDVI indices value ($NDVI_{Built-up} < 0.2$, $NDVI_{Bare\ land} < 0.2$, $NDVI_{Vegetation} > 0.2$, $NDVI_{Water} < 0$) recommended by Chen et al. (2006) for different LULC types.

3.3 Relationship between LULC and LST

LULC significantly affects LST. Transformations between different LULC types (especially urban expansion) increase the effect of UHI by increasing and strong effect on the number and distribution of hot spots (Tran et al. 2017). The LST

distribution map was prepared based on the classification scheme of the standard deviation (Weng et al. 2004) using digital images in the thermal band (DN 0–255) of Landsat TM/ETM+ /OLI images for the study area (Fig. 4). The mean LST values associated with LULC categories were summarized in Table 5. It was observed that during 1989, 1999 and 2015, the temperature changed in the 20 °C–50 °C, 21 °C–45 °C and 22 °C–50 °C range, respectively. The urban built-up had the highest average temperature, followed by bare land, agricultural land, vegetation and water in 1989, 1999 and 2015, respectively and highest average temperatures were observed for all the LULC categories in 1989 (Fig. 5a). The
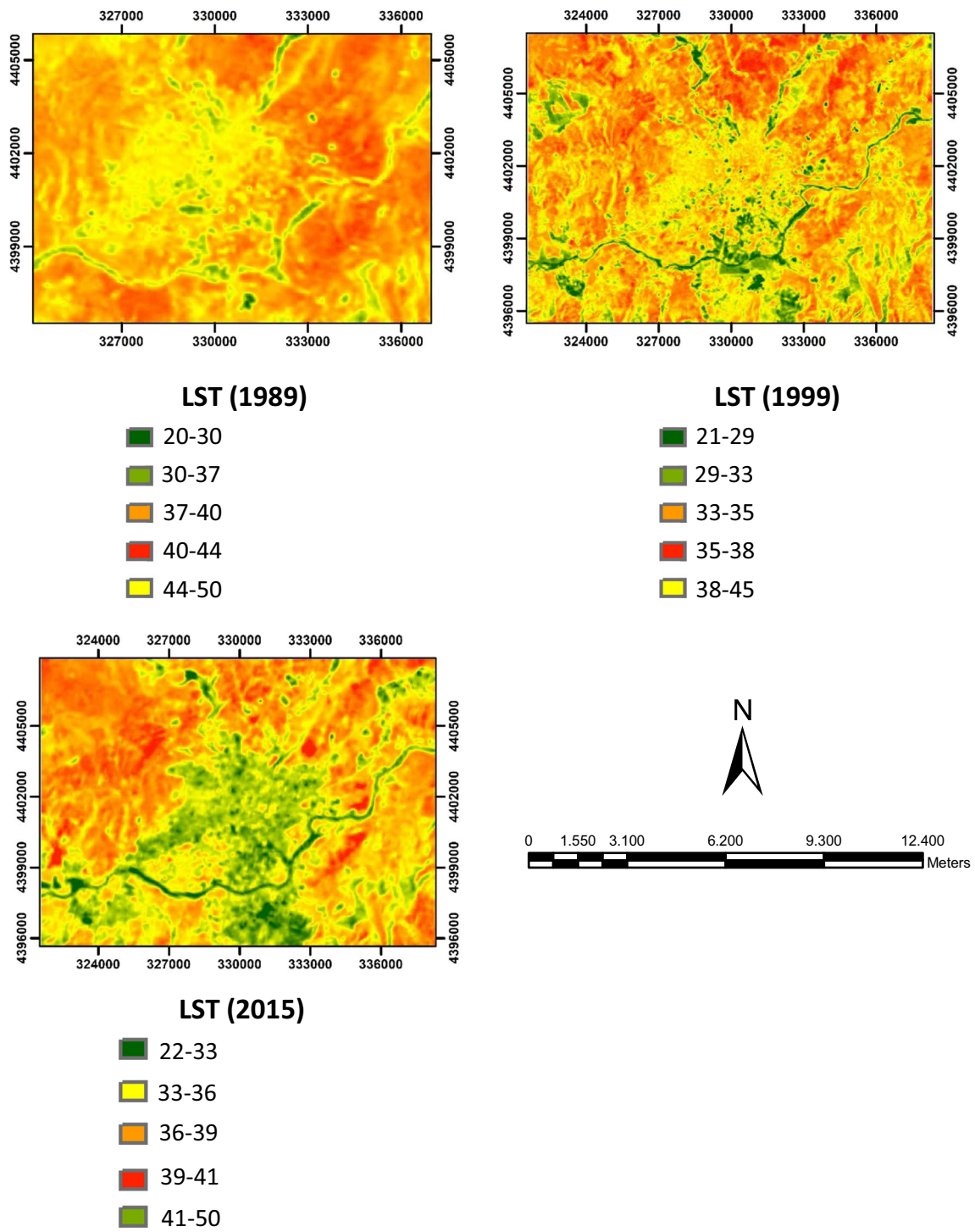
Fig. 4 Spatial distribution of LST (in Celsius) within study area

Table 5 LST statistic values for Landsat images used in this study

Image acquired	Max temp (°C)	Min temp (°C)	Mean temp (°C) (μ)	St. deviation (°C) (δ)	$\mu + (0.5 \times \delta)$
1989	49.81	21.25	37.20	2.77	38.58
1999	45.71	21.80	37.85	2.95	39.32
2015	50.14	22.30	38.55	3.28	40.19
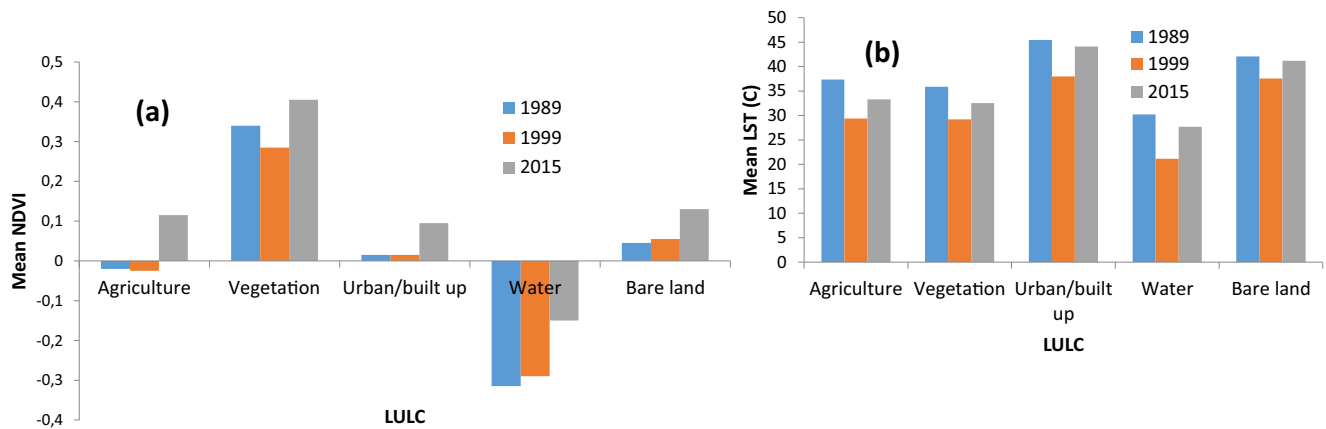
Fig. 5 Graphical representation of mean NDVI (**a**) and mean LST (**b**) with different LULC during the study period (Gaylan 2017)

average LST values for urban built-up were 44.10 °C, 37.99 °C, and 42.30 °C in 1989, 1999, and 2015, respectively. The LST of urban built-up had a 6.11 °C decrease from 1989 to 1999 but increased by the maximum LST difference of 4.31 °C between 1999 and 2015. The bare land had the second highest LST followed by agricultural land over the study period for all the LULC categories. The LST of barren land had a 4.53 °C decrease from 1989 to 1999 but did not change significantly between 1989 and 2015. The LST for agricultural land was 37.33 °C in 1989, and changed to 29.38 and 33.28 °C in 1999 and 2015, respectively. The LST of agricultural land had a 4.05 °C decrease while the increase in urban built-up area was 12.35% from 1989 to 2015. The LST of vegetated areas had a 6.65 °C decrease from 1989 to 1999, but increased by 3.34 °C between 1999 and 2015. The lowest LST was observed for all the LULC categories in 1999 and water body and an area covered by green vegetation contains had the lowest average temperature for all the years. There is a maximum LST difference of 16.82 °C between urban built-up and water body in 1999. The average temperature increased from 1999 to 2015 and the average temperature increased from 1989 to 1999 for all the LULC categories (Fig. 5b). Generally, there was no great change in LST between 1989 and 2015.

Based on August, the areas determined as agricultural areas within the study area were considered as harvested areas. These areas are also considered as bare land. Studies done by Pu et al. (2006) and Zareie et al. (2016) have shown that

the LST values of bare land are higher than the LST values of urban areas. Similar results were obtained in our study. The high LST values in these areas can vary depending on the content of the soil (sand, clay, etc.). The LST values on the dates of satellite images are not dependent on the spatial values of the land use classes, but may depend on the average daily air temperature on the satellite images taken. Temperature measurements should be performed on different LULC properties based on field observations to show how LST results calculated from Landsat TM/ETM thermal band have been verified with actual field surface temperatures (Mallick et al. 2008). As a matter of fact, the daily mean air temperatures of the dates indicated by the LST values stated on the date (the average daily air temperature at 27.08.1989 is 24,1 °C, the daily average air temperature at 07.08.1999 is 19,0 °C, the daily mean air temperature at 11.08.2015 is 23,7 °C) parallel to each other.

Distorted construction resulting from urban growth decreases the amount of leakage of rain water into the soil, whereas surface flows increase. Therefore, underground water levels are decreasing and the amount of groundwater is gradually decreasing. Depending on these two factors, the evapotranspiration (evaporation + sweating) event required for the hydrological cycle (water cycle) is not sufficiently realized. As a result, the water balance deteriorates and this leads to climate change (Yüksel et al. 2011). And so the changes in land use also affect the climate elements such as daily max and min
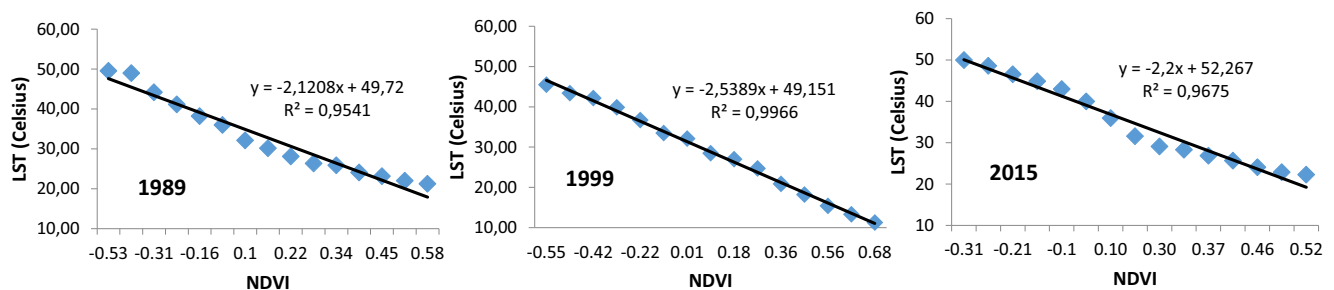

Fig. 6 Linear relationship between NDVI and LST

Table 6 UHI intensity values which calculated during the study period (adapted from Hala Adel Effat, 2014)

Image acquired	Urban LST (°C)			Rural LST (°C)			
	Max temp (°C)	Min temp (°C)	Mean temp (°C) (μ)	Max temp (°C)	Min temp (°C)	Mean temp (°C) (μ)	UHI intensity (°C) (μ$_{Urban}$ − μ$_{Rural}$)
1989	49.81	38.58	44.10	42.21	32.45	37.33	6.77
1999	45.71	39.32	37.99	39.56	29.21	34.38	3.61
2015	50.14	40.19	42.30	42.84	23.72	33.28	9.02

temperature. Land use change causes aerosol emissions and surface albedo changes. For this reason, land use change is one of the basic human activities that may disrupt the radiation balance of the Earth (Myhre and Myhre 2003). For example; air temperature has declined due to the transformation of water-marsh land uses into agricultural lands with high albedo values (Gophen 2014).

3.4 Relationship between LST and NDVI

NDVI and LST had a strong correlation (Kaufmann et al. 2003; Chen et al. 2006) and it was clearly seen that there was an increase in NDVI values (greater proportion of vegetation) during the summer (Julien et al. 2006). The increase in LST values was observed together with a reduction in NDVI values (Bokaie et al. 2016). There is a significant and negative relationship between vegetated land (having very low temperatures) and LST (Li et al. 2014). The surface temperature can be expressed using linear regression between surface temperature and NDVI (Fig. 6) according to certain acceptable range accuracy (Zareie et al. 2016a, 2016b). The coefficients (R^2) were 0.95, 0.99 and, 0.96, respectively and this R^2 value was an indicative of the strong relationship between LST and NDVI when the correlation made between NDVI and LST was considered. A negative correlation was determined between both parameters when a general assessment was made between NDVI values and LST values (Lo et al. 1997; Kaplan et al. 2018) based on the information in the literature during the study period (Fig. 6).

Areas covered by the highest NDVI values are located in south, southwest and north of the Sivas city center. The lowest NDVI values concentrated in an area covering the central city of Sivas and its surroundings. Areas covered by the highest NDVI values are usually forested areas (Fig. 3). NDVI values increased with the increase of vegetated areas and LST values decreased. On the other hand, an increase in LST was determined by increasing agricultural land and a decrease in LST was determined by decreasing bare land whereas without much change in NDVI values between 1989 and 2015. When an assessment was made for urban areas and bare land for 1989 and 2015, it was observed that LST was decreased by increasing NDVI. According to the research results obtained

by Yuan and Bauer (2007), NDVI may be used for analysis of surface UHI effects during summer. Vegetation plays major role to reduce the amount of thermal radiation (Chakraborty et al. 2014).

3.5 Intensity of Urban Heat Island

A procedure is applied based on the Eq. (5) in order to calculate the intensity of UHI. UHI intensity calculated using the mean temperature (μ) and standard deviation (δ) values of LST statistics for the specified year. The mean temperatures were 37.20 °C, 37.85 °C, and 38.55 °C in 1989, 1999, and 2015, respectively (Table 5).

The UHI intensity were 6.77 °C, 3.61 °C, and 9.02 °C in 1989, 1999, and 2015, respectively. The UHI intensity had a 3.16 °C decrease from 1989 to 1999 but increased by the UHI intensity difference of 5.41 °C between 1999 and 2015. It has been noticed that UHI intensity had a 2.25 °C increase when the general assessment made between 1989 and 2015 and it has showed that a fluctuating trendof UHI intensity. The mean temperatures revealed a positive UHI intensity due to the lowest mean temperatures that were recorded in the urban area when compared to the mean temperatures in urban and rural areas (Table 6).

4 Conclusion

This study examined the effects of LU change on LST and UHI intensity, which were determined for the Sivas city center and its surroundings from 1989 to 2015, using Landsat satellite images. Accuracy analysis results revealed obviously that the accuracy of the classification according to our study also supported to previous studies. When an assessment was made on obtained results, it was seen that the urban built-up areas and agricultural lands increased while barren land decreased over the study period. The main reason for the increase in agricultural and urban areas is the transition to city residential settlements from villages. The vegetated areas decreased from 1989 to 1999, whereas they increased from 1999 to 2015. Agricultural and bare land are the dominant LU classes in the study area. The importance of agricultural activity is great

on the interpretation of LULC categories (Chen et al. 2006). When examining changes in LU, a majority of bare land (approximately 12.35%) have been converted to urban built-up area. The city of Sivas has grown mainly towards the northeast, south and south-west. Part of the agricultural land in the study area has also turned into residential area. When increasing development of settlement areas towards the Kızılırmak River is taken into consideration, it has been deemed that this situation might present a threat to the river. Such drawbacks can be observed as a result of population pressure on the land and inadequate land use planning.

The liberal economic policies adopted in Turkey since 1950 and the mechanization of agriculture have accelerated the migration from rural to urban areas. As a result, the urban population has increased steadily to daylight. Especially in the years 1980 and after 1980, the rapid growth of the scale in the cities gave birth to the result. With the 1980s, approaches have been adopted aiming to bring the areas that lost their function in the city center to the urban economy (Yedekci 2015). In line with these explanations, the period of time when the urban growth is the most in the city center of Sivas is striking as 1999–2015 compared to the interval between 1989 and 1999. In parallel with this increase seen in the overall Turkish cities, a similar increase was determined in Sivas city center. Population growth between 1999 and 2015 also supported urban growth.

With the investigated relationship between LULC, NDVI and LST, the spatial distribution maps of NDVI and LST were created carefully. When changes in LULC were accompanied by changes in NDVI and LST, the higher NDVI values were found surprisingly to be over the dense vegetation areas and the urban built-up land had the highest average temperature over the study period. A negative correlation was determined between NDVI and LST, and a lower average LST was observed in vegetated areas. The differences in air temperature on the date of receipt of satellite images had led to the different surface temperature values. Urban built-up land, particularly with an average temperature of 44.10 °C (1989), are the hottest places while water bodies with an average temperature of 27.68 °C (2015) are the coolest places. Urban built-up and bare lands have the highest LST in the study area. The urban built-up areas have a higher surface temperature than the agricultural land due to the city's unique geographical location, physical and morphological structure and mainly depending on the construction material.

It is generally known that industrial and residential areas are factories which contribute to the development of UHI. The urban built-up areas increased but on the other hand a positive UHI intensity was occurred. The obtained results have clearly shown there was increase in urban areas, in parallel with the intensity of UHI in the study area was an increase tendency between 1989 and 2015. Because of the urban temperature is higher than rural temperature, an urban heat island formation was determined for the Sivas city center and its surroundings.

Urban heat islands have led to negative effects such as health problems, increase in energy consumption, air pollution and water shortage (Agarwal and Tandon 2010; Amanollahi et al. 2013). According to the results obtained from our research, Sivas is a city that poses a problem in terms of urban heat island and similar problems. As a result, planning studies should be carried out carefully taking into consideration the natural capacities of the land in order to prevent its misuse, and the government should take the necessary measures immediately in the region with the urban heat island.

Compliance with Ethical Standards

Disclosure The authors of the manuscript solemnly declare that no scientific and/or financial conflicts of interest, exists with other people or institutions.

References

Alonso, M.S., Fidalgo, M.R., Labajo, J.L.: The urban heat island in Salamanca (Spain) and its relationship to meteorological parameters. Clim. Res. **34**, 39–46 (2007)

Amanollahi, J., Tzanis, C., Abdullah, A.M., Ramli, M.F., Pirasteh, S.: Development of the models to estimate particulate matter from thermal infrared band of Landsat enhanced thematic mapper. Int. J. Environ. Sci. Technol. **10**, 1245–1254 (2013)

Amanollahi, J., Tzanis, C., Ramli, M.F., Abdullah, A.M.: Urban heat evolution in a tropical area utilizing Landsat imagery. Atmos. Res. **167**, 175–182 (2016)

Agarwal, M., Tandon, A.: Modeling of the urban heat island in the form of mesoscale wind and of its effect on air pollution dispersal. Appl. Math. Model. **34**, 2520–2530 (2010)

Anderson, J. R., E. E. Hardy, J. T. Roach, and R. E. Witmer, 1976: A land use and land cover classification system for use with remote sensor data. US government printing office. *DC: U.S. Geological Survey. No. Professional Paper 964*, Washington

Bagan, H., Takeuchi, W., Kinoshita, T., Bao, Y., Yamagata, Y.: Land cover classification and change analysis in the Horqin sandy land from 1975 to 2007. IEEE J Sel Top Appl Earth Obs Remote Sens. **3**(2), 168–177 (2010)

Bagan, H., Yamagata, Y.: Landsat analysis of urban growth: how Tokyo became the world's largest megacity during the last 40 years. Remote Sens. Environ. **127**, 210–222 (2012)

Bakr, N., Weindorf, D.C., Bahnassy, M.H., Marei, S.M., Badawi, M.M.E.: Monitoring land cover changes in a newly reclaimed area of Egypt using multi-temporal Landsat data. Appl. Geogr. **30**, 592–605 (2010)

Balcik, F.B.: Determining the impact of urban components on land surface temperature of Istanbul by using remote sensing indices. Environ. Monit. Assess. **186**(2), 859–872 (2014)

Bokaie, M., Zarkesh, M.K., Arasteh, P.D., Hosseini, A.: Assessment of urban heat island based on the relationship between land surface temperature and land use/ land cover in Tehran. Sustain. Cities Soc. **23**, 94–104 (2016)

Butt, A., Shabbir, R., Ahmad, S.S., Aziz, N.: Land use change mapping and analysis using remote sensing and GIS: a case study of Simly watershed, Islamabad, Pakistan. Egyptian J Remote Sens Space Sci. **18**, 251–259 (2015)

Carlson, T.N., Ripley, D.A.: On the relation between NDVI, fractional vegetation cover, and leaf area index. Remote Sens. Environ. **62**, 241–252 (1997)

Chakraborty, S.D., Kant, Y., Bharath, B.D.: Study of land surface temperature in Delhi city to managıng the thermal effect on urban developments. Int J Advanced Sci Tech Res. **4**(1), 439–450 (2014)

Chakraborty, S.D., Kant, Y., Mitra, D.: Assessment of land surface temperature and heat fluxes over Delhi using remote sensing data. J. Environ. Manag. **148**, 143–152 (2015)

Chaudhuri, G., Mishra, N.B.: Spatio-temporal dynamics of land cover and land surface temperature in Ganges-Brahmaputra delta: a comparative analysis between India and Bangladesh. Appl. Geogr. **68**, 68–83 (2016)

Chen, X.L., Zhao, H.M., Li, P.X., Yin, Z.Y.: Remote sensing image-based analysis of the relationship between urban heat island and land use/ cover changes. Remote Sens. Environ. **104**(2), 133–146 (2006)

Chen, Y.C., Chiu, H.W., Su, Y.F., Wu, Y.C., Cheng, K.S.: Does urbanization increase diurnal land surface temperature variation? Evidence and implications. Landsc. Urban Plan. **157**, 247–258 (2017)

Cheung, H.K.W.: An Urban Heat Island Study for Building and Urban Design, a Thesis Submitted to The University Of Manchester for the Degree of Doctor of Philosophy in the Faculty of Engineering and Physical Sciences. School of Mechanical, Aerospace and Civil Engineering (2011)

Churches, C.E., Wampler, P.J., Sun, W., Smith, A.J.: Evaluation of forest cover estimates for Haiti using supervised classification of Landsat data. Int. J. Appl. Earth Obs. Geoinf. **30**, 203–216 (2014)

Congalton, R.G.: A review of assessing the accuracy of classifications of remotely sensed data. Remote Sens. Environ. **37**(1), 35–46 (1991)

Deosthali, V.: Impact of rapid urban growth on heat and moisture islands in Pune City, India. Atmos. Environ. **34**, 2745–2754 (2000)

Dhalluin, A., Bozonnet, E.: Urban heat islands and sensitive building design-a study in some French cities context. Sustain. Cities Soc. **19**, 292–299 (2015)

Ding, F., Xu, H.Q.: Comparison of three algorithms for retrieving land surface temperature from Landsat TM thermal infrared band. J Fujian Norm Univ (Nat Sci Ed). **24**(1), 91–96 (2008)

Du, M., Wang, Q., Cai, G.: Temporal and spatial variations of urban heat island effect in Beijing using ASTER and TM data. In Urban Remote Sensing Event. 1–5 (2009)

Effat, H.A., Hassan, O.A.K.: Change detection of urban heat islands and some related parameters using multi-temporal Landsat images; a case study for Cairo city, Egypt. Urban Climate. **10**, 171–188 (2014)

Effat, H.A., Taha, L.G.E., Mansour, K.F.: Change detection of land cover and urban heat islands using multi-temporal landsat images, application in Tanta City, Egypt. Open J Remote Sens Positioning. **1**(2), 1–15 (2014)

Efstathiou, M.N., Varotsos, C.A., Singh, R.P., Cracknell, A.P., Tzanis, C.: On the longitude dependence of total ozone trends over middle-latitudes. Int. J. Remote Sens. **24**, 1361–1367 (2003)

EPA, 2008: Urban Heat Island basics. In Reducing Urban Heat Islands: Compendium of Strategies; Chapter 1; Draft Report, United States Environmental Protection Agency: Washington, DC, USA. Available online: http://www.epa.gov/heatisland/resources/ compendium.htm (accessed on June 2018)

FAO, 1997: Estimating Biomass and Biomass Change in Tropical Forests. Food and Agriculture Organization of the United Nations. http://www.fao.org/docrep/W4095E/W4095E00.htm. Accessed July, 2018

Feng, H., Liu, H., Wu, L.: Monitoring the relationship between the land surface temperature change and urban growth in Beijing, China. IEEE J. Select. Top. Appl. Earth Observ. Rem. Sens. **7**(10), 4010–4019 (2014)

Fu, P., Weng, Q.: A time series analysis of urbanization induced land use and land cover change and its impact on land surface temperature with Landsat imagery. Remote Sens. Environ. **175**, 205–214 (2016)

Gandhi, G.M., Parthiban, S., Thummalu, N., Christy, A.: NDVI: vegetation change detection using remote sensing and gis – a case study of Vellore District. Procedia Comput Sci. **57**, 1199–1210 (2015)

Gaylan, F.G.: Urban land use land cover changes and their effect on land surface temperature: case study using Dohuk City in the Kurdistan region of Iraq. Climate. **5**(1), 3 (2017)

GCM: 1/25.000 scale digital topographic map of the study area. National Defense Department General Command of Mapping, Ankara (2005)

GDMRE, 1997: Environmental geology and natural resources of Sivas city. General Directorate of Mineral Research and Exploration, Central Anatolia 1st Regional Directorate Geological Studies Directorate 168p, Sivas

GDMRE: 1/25.000 scale digital geology map of the study area. General Directorate of Mineral Research and Exploration, Ankara (2005)

GEOG, 2016: Department of Geography. PennState College of Earth and Mineral Sciences, Remote Sensing Analysis and Applications https://www.e-education.psu.edu/geog883/node/524. Accessed 25 June 2018

Ghebrezgabher, M.G., Yang, T., Yang, X., Wang, X., Khan, M.: Extracting and analyzing forest and woodland cover change in Eritrea based on landsat data using supervised classification. Egypt J Remote Sens Space Sci. **19**, 37–47 (2016)

Gophen, M.: Land-use, albedo and air temperature changes in the hula valley (Israel) during 1946-2008. Open J Mod Hydrol. **4**(04), 101–111 (2014)

Guo, G., Zhou, X., Wu, Z., Xiao, R., Chen, Y.: Characterizing the impact of urban morphology heterogeneity on land surface temperature in Guangzhou, China. Environ. Model Softw. **84**, 427–439 (2016)

Hansen, H.S.: Modelling the future coastal zone urban development as implied by the IPCC SRES and assessing the impact from sea level rise. Landsc. Urban Plan. **98**, 141–149 (2010)

Hegazy, I.R., Kaloop, M.R.: Monitoring urban growth and land use change detection with GIS and remote sensing techniques in Daqahlia governorate Egypt. Int J Sustain Built Environ. **4**, 117–124 (2015)

Heinl, M., Hammerle, A., Tappeiner, U., Leitinger, G.: Determinants of urban-rural land surface temperature differences-a landscape scale perspective. Landsc. Urban Plan. **134**, 33–42 (2015)

Herold, M., Goldstein, N.C., Clarke, K.C.: The spatiotemporal form of urban growth: measurement, analysis and modeling. Remote Sens. Environ. **86**, 286–302 (2003)

Hove, L. W. A. V., G. J. Steeneveld, C. M. J. Jacobs, B. G. Heusinkveld, J. A. Elbers, E. J. Moors, and A. A. M. Holtslag, 2011: Exploring the urban heat island intensity of Dutch cities. Alterra report 2170 Alterra, part of Wageningen UR Wageningen

Imhoff, M.L., Zhang, P., Wolfe, R.E., Bounoua, L.: Remote sensing of the urban heat island effect across biomes in the continental USA. Remote Sens. Environ. **114**, 504–513 (2010)

Ji, X., Niu, X.: The attribute accuracy assessment of land cover date in the national geography conditions survey. ISPRS Ann. Photogramm. Remote Sens. Spatial Inf. Sci. **2**(4), 35–40 (2014)

Jiang, Y., Fu, P., Weng, Q.: Assessing the impacts of urbanization-associated land use/cover change on land surface temperature and surface moisture: a case study in the midwestern United States. Remote Sens. **7**(4), 4880–4898 (2015)

Johansen, B., Tømmervik, H.: The relationship between phytomass, NDVI and vegetation communities on Svalbard. Int. J. Appl. Earth Obs. Geoinf. **27**, 20–30 (2014)

Julien, Y., Sonrino, J.A., Verhoef, W.: Changes in land surface temperatures and NDVI values over Europe between 1982 and 1999. Remote Sens. Environ. **103**, 43–55 (2006)

Kaplan, G., Avdan, U., Avdan, Z.Y.: Urban heat island analysis using the Landsat 8 satellite data: a case study in Skopje, Macedonia. In Multidisciplinary Digital Publishing Institute Proceedings. **2**(7), 58 (2018)

Karakus, C.B., Kavak, K.S., Cerit, O.: Determination of variations in land cover and land use by remote sensing and geographic information systems around the city of Sivas (Turkey). Fresenius Environ. Bull. **23**(3), 667–677 (2014)

Kaufmann, R.K., Zhou, L., Myneni, R.B., Tucker, C.J., Slayback, D., Shabanov, N.V., Pinzon, J.: The effect of vegetation on surface temperature: a statistical analysis of NDVI and climate data. Geophys. Res. Lett. **30**(22), 2137 (2003)

Kaya, S., Basar, U.G., Karaca, M., Seker, D.Z.: Assessment of urban heat islands using remotely sensed data. Ecology. **21**(84), 107–113 (2012)

Kumar, D., Shekhar, S.: Statistical analysis of land surface temperature–vegetation indexes relationship through thermal remote sensing. Ecotoxicol. Environ. Saf. **121**, 39–44 (2015)

Kumar, K.S., Bhaskar, P.U., Padmakumarı, K.: Estimation of land surface temperature to study urban heat island effect using Landsat ETM+ image. Int J Eng Sci Technol (IJEST). **4**(2), 771–778 (2012)

Lambin, E.F., Rounsevell, M.D.A., Geist, H.J.: Are agricultural land-use models able to predict changes in land-use intensity? Agric. Ecosyst. Environ. **82**, 321–331 (2000)

Landsat Project Science Office, 2002: Landsat 7 Science Data user's Handbook. Washington, DC, Goddard Space Flight Center, NASA. http://ltpwww.gsfc.nasa.gov/IAS/handbook/handbook_toc.html. Accessed 13 May 2018

Landsat Project Science Office, 2016: Landsat 8 science data user's handbook. Retrieved 13 September 2016, fromhttps://landsat.usgs.gov/documents/Landsat8DataUsersHandbook.pdf. Accessed 13 May 2018

Lee, T.W., Lee, J.Y., Wang, Z.H.: Scaling of the urban heat island intensity using time-dependent energy balance. Urban Climate. **2**, 16–24 (2012)

Leong, Y.P., Chng, L.K., Ong, J., Choo, C.M., Laili, N.: Preliminary study of the impacts of land use and land cover change on land surface temperature with remote sensing technique: a case study of the Klang Valley and Penang Island, Malaysia. Segi. **9**, 5–29 (2015)

Li, W., Bai, Y., Chen, Q., Hee, K., Ji, X., Han, C.: Discrepant impacts of land use and land cover on urban heat islands: a case study of Shanghai, China. Ecol. Indic. **47**, 171–178 (2014)

Li, Y., Zhang, H., Kainz, W.: Monitoring patterns of urban heat islands of the fast-growing Shanghai metropolis, China: using time-series of Landsat TM/ETM+ data. Int. J. Appl. Earth Obs. Geoinf. **19**, 127–138 (2012)

Liu, T., Yang, X.: Monitoring land changes in an urban area using satellite imagery, GIS and landscape metrics. Appl. Geogr. **56**, 42–54 (2015)

Liu, Y., Huang, X., Yang, H., Zhong, T.: Environmental effects of land-use/cover change caused by urbanization and policies in Southwest China karst area-a case study of Guiyang. Habitat Int. **44**, 339–348 (2014)

Lo, C.P., Quattrochi, D.A.: Land-use and land-cover change, urban heat island phenomenon, and health implications: a remote sensing approach. Photogramm. Eng. Remote Sens. **69**(9), 1053–1063 (2003)

Lo, C.P., Quattrochi, D.A., Luvall, J.C.: Application of high-resolution thermal infrared remote sensing and GIS to assess the urban heat island effect. Int. J. Remote Sens. **18**, 287–303 (1997)

Lu, D., Weng, Q.: A survey of image classification methods and techniques for improving classification performance. Int. J. Remote Sens. **28**(5), 823–870 (2007)

Ma, Y., Kuang, Y., Huang, N.: Coupling urbanization analyses for studying urban thermal environment and its interplay with biophysical parameters based on TM/ETM+ imagery. Int. J. Appl. Earth Obs. Geoinf. **12**(2), 110–118 (2010)

Mahiroğulları, A. M., 2003: Today's City of Sivas Dating Back to Ancient Times. Typography Sivas, 199p

Malaret, E., Bartolucci, L.A., Lozano, D.F., Anuta, P.E., McGillem, C.D.: Landsat-4 and Landsat-5 thematic mapper data quality analysis. Photogramm. Eng. Remote Sens. **51**, 1407–1416 (1985)

Mallick, J., Kant, Y., Bharath, B.D.: Estimation of land surface temperature over Delhi using Landsat-7 ETM+. J Indian Geophys Union. **12**(3), 131–140 (2008)

Mathew, A., Khandelwal, S., Kaul, N.: Spatial and temporal variations of urban heat island effect and the effect of percentage impervious surface area and elevation on land surface temperature: study of Chandigarh City, India. Sustain. Cities Soc. **26**, 264–277 (2016)

Mei, A., Manzo, C., Fontinovo, G., Bassani, C., Allegrini, A., Petracchini, F.: Assessment of land cover changes in Lampedusa Island (Italy) using Landsat TM and OLI data. J. Afr. Earth Sci. **122**, 15–24 (2016)

Melesse, A.M.: Spatiotemporal dynamics of land surface parameters in the Red River of the North Basin. Phys. Chem. Earth. **29**, 795–810 (2004)

Mirzaei, P.A., Haghighat, F., Nakhaie, A.A., Yagouti, A., Giguère, M., Keusseyan, et al.: Indoor thermal condition in urban heat island-development of a predictive tool. Build. Environ. **57**, 7–17 (2012)

Mohan, M., Kandya, A.: Impact of urbanization and land-use/land-cover change on diurnal temperature range: a case study of tropical urban airshed of India using remote sensing data. Sci. Total Environ. **506**, 453–465 (2015)

Mundia, C.N., Aniya, M.: Analysis of land use/cover changes and urban expansion of Nairobi City using remote sensing and GIS. Int. J. Remote Sens. **26**, 2831–2849 (2005)

Myhre, G., Myhre, A.: Uncertainties in radiative forcing due to surface albedo changes caused by land-use changes. J. Clim. **16**, 1511–1524 (2003)

Odindi, J.O., Bangamwabo, V., Mutanga, O.: Assessing the value of urban green spaces in mitigating multi-seasonal urban heat using MODIS land surface temperature (LST) and Landsat 8 data. Int J Environ Res. **9**(1), 9–18 (2015)

Oke, T.R.: City size and the urban heat island. Atmos. Environ. **7**, 769–779 (1973)

Omran, E.S.E.: Detection of land-use and surface temperature change at different resolutions. J. Geogr. Inf. Syst. **4**, 189–203 (2012)

Ozesmi, S.L., Bauer, M.E.: Satellite remote sensing of wetlands. Wetl. Ecol. Manag. **10**, 381–402 (2002)

Pegau, W.S., Paulson, C.A.: The albedo of Arctic leads in summer. Ann. Glaciol. **33**, 221–224 (2001)

Peng, S., Piao, S., Ciais, P., Friedlingstein, P., Ottle, C., Bréon, F.M., Nan, H., Zhou, L., Myneni, R.B.: Surface urban heat island across 419 global big cities. Environ Sci Technol. **46**, 696–703 (2012)

Pu, R., Gong, P., Michishita, R., Sasagawa, T.: Assessment of multi-resolution and multi-sensor data for urban surface temperature retrieval. Remote Sens. Environ. **104**, 211–225 (2006)

Ramachandra, T.V., Kumar, U.: Urban land surface temperature with land cover dynamics: multi-resolution, spatio-temporal data analysis of greater Bangalore. Int J Geoinformatics. **5**(3), 43–53 (2009)

Raynolds, M.K., Comiso, J.C., Walker, D.A., Verbyla, D.: Relationship between satellite-derived land surface temperatures, arctic vegetation types, and NDVI. Remote Sens. Environ. **112**, 1884–1894 (2008)

Rembold, F., Carnicelli, S., Nori, M., Ferrari, G.A.: Use of aerial photographs, Landsat TM imagery and multidisciplinary field survey for land-cover change analysis in the lakes region. Int. J. Appl. Earth Obs. Geoinf. **2**(3–4), 181–189 (2000)

Saadat, H., Adamowski, J., Bonnell, R., Sharifi, F., Namdar, M., Ebrahim, S.A.: Land use and land cover classification over a large area in Iran based on single date analysis of satellite imagery. ISPRS J. Photogramm. Remote Sens. **66**, 608–619 (2011)

Sajikumar, N., Remya, R.S.: Impact of land cover and land use change on runoff characteristics. J. Environ. Manag. **161**, 460–468 (2015)

Schneider, A., Woodcock, C.E.: Compact, dispersed, fragmented, extensive? A comparison of urban growth in twenty-five global cities using remotely sensed data, pattern metrics and census information. Urban Stud. **45**(3), 659–692 (2008)

Schultz, P.A., Halpert, M.S.: Global correlation of temperature, NDVI and precipitation. Adv. Space Res. **13**(5), 277–280 (1993)

Sekertekin, A.İ., Kutoglu, S.H., Kaya, S.: Evaluation of spatio-temporal variability in land surface temperature: a case study of Zonguldak, Turkey. Environ. Monit. Assess. **188**(1), 1–15 (2016)

Shahmohamadi, P., Ani, A.I.C., Ramly, A., Maulud, K.N.A., Nor, M.F.I.M.: Reducing urban heat island effects: A systematic review to achieve energy consumption balance. Int J Phys Sci. **5**(6), 626–636 (2010)

Shalaby, A., Tateishi, R.: Remote sensing and GIS for mapping and monitoring land cover and land use changes in the northwestern coastal zone of Egypt. Appl. Geogr. **27**, 28–41 (2007)

Shen, G., Ibrahim, A.N., Wang, Z., Ma, C., Gong, J.: Spatial–temporal land-use/land-cover dynamics and their impacts on surface temperature in Chongming Island of Shanghai, China. Int. J. Remote Sens. **36**(15), 4037–4053 (2015)

Silleos, N.G., Alexandridis, T.K., Gitas, I.Z., Perakis, K.: Vegetation indices: advances made in biomass estimation and vegetation monitoring in the last 30 years. Geocarto Int. **21**(4), 21–28 (2006)

Sinha, S., Sharma, L.K., Nathawat, M.S.: Improved land-use/land-cover classification of semi-arid deciduous forest landscape using thermal remote sensing. Egypt J Remote Sens Space Sci. **18**, 217–233 (2015)

Sivas Governorship, 2006: Sivas 2023 Strategic Provincial Development Plan. T.C. Governorship of Sivas Provincial Social and Economic Planning Center Sivas, 291p

Streutker, D.R.: A remote sensing study of the urban heat island of Houston, Texas. Int. J. Remote Sens. **23**(13), 2595–2608 (2002)

Tran, D.X., Pla, F., Latorre-Carmona, P., Myint, S.W., Caetano, M., Kieu, H.V.: Characterizing the relationship between land use land cover change and land surface temperature. ISPRS J. Photogramm. Remote Sens. **124**, 119–132 (2017)

Trenberth, K.E., Jones, P.D., Ambenje, P., Bojariu, R., Easterling, D., Tank, A.K., Parker, D., Rahimzadeh, F., Renwick, J.A., Rusticucci, M., Soden, B., Zhai, P.: Observations: surface and atmospheric climate change. In: Solomon, S., Qin, D., Manning, M., Chen, Z., Marquis, M., Averyt, K.B., Tignor, M., Miller, H.L. (eds.) Climate Change 2007: The Physical Science Basis. Contribution of Working Group Ito the Fourth Assessment Report of the Intergovernmental Panel on Climate Change. Cambridge University Press (2007)

Trlica, A., Hutyra, L.R., Schaaf, C.L., Erb, A., Wang, J.A.: Albedo, land cover, and daytime surface temperature variation across an urbanized landscape. Earth's Future. **5**(11), 1084–1101 (2017)

TUIK, 2015: Turkish statistical institute, results of population censuses. 1935-2000 and results of address based population registration system (2007-2015)

United Nations, 2014: Population division world urbanization prospects. United Nations, Department of Economic and Social Affairs, the 2014 revision

Varotsos, C.: The southern hemisphere ozone hole split in 2002. Environ. Sci. Pollut. R. **9**, 375–376 (2002)

Varotsos, C.A., Melnikova, I.N., Cracknell, A.P., Tzanis, C., Vasilyev, A.V.: New spectral functions of the near-ground albedo derived from aircraft diffraction spectrometer observations. Atmos. Chem. Phys. **14**(13), 6953–6965 (2014)

Wang, S., Ma, Q., Ding, H., Liang, H.: Detection of urban expansion and land surface temperature change using multi-temporal landsat images. Resour. Conserv. Recycl. **128**, 526–534 (2016)

Wardlow, B.D., Kastens, J.H., Egbert, S.L.: Using USDA crop progress data for the evaluation of Greenup onset date calculated from MODIS 250 meter data. Photogramm. Eng. Remote. Sens. **72**, 1225–1234 (2006)

Weng, Q.: Thermal infrared remote sensing for urban climate and environmental studies: methods, applications, and trends. ISPRS J. Photogramm. Remote Sens. **64**(4), 335–344 (2009)

Weng, Q., Lu, D., Schubring, J.: Estimation of land surface temperature–vegetation abundance relationship for urban heat island studies. Remote Sens. Environ. **89**, 467–483 (2004)

Wondrade, N., Dick, Q.B., Tveite, H.: GIS based mapping of land cover changes utilizing multi-temporal remotely sensed image data in Lake Hawassa watershed, Ethiopia. Environ. Monit. Assess. **186**(3), 1765–1780 (2014)

Xian, G., Crane, M.: An analysis of urban thermal characteristics and associated land cover in Tampa Bay and Las Vegas using Landsat satellite data. Remote Sens. Environ. **104**, 147–156 (2006)

Xiao, H., Weng, Q.: The impact of land use and land cover changes on land surface temperature in a karst area of China. J. Environ. Manag. **85**(1), 245–257 (2007)

Xu, H., Ding, F., Wen, X.: Urban expansion and heat island dynamics in the Quanzhou region, China. IEEE J Sel Top Appl Earth Obs Remote Sens. **2**(2), 74–79 (2010)

Yang, J., Wong, M.S., Menenti, M., Nichol, J.: Study of the geometry effect on land surface temperature retrieval in urban environment. ISPRS J. Photogramm. Remote Sens. **109**, 77–87 (2015)

Yedekci, G., 2015: Urban transformation with the examples applied in the world and Turkey and the original conversion model proposal. *Architecture Foundation Economic Business Publications*, ISBN 978-605- 86645-6-2, Istanbul

Yuan, F., Bauer, M.E.: Comparison of impervious surface area and normalized difference vegetation index as indicators of surface urban heat island effects in Landsat imagery. Remote Sens. Environ. **106**, 375–386 (2007)

Yuan, F., Sawaya, K.E., Loeffelholz, B.C., Bauer, M.E.: Land cover classification and change analysis of the twin cities (Minnesota) metropolitan area by multitemporal landsat remote sensing. Remote Sens. Environ. **98**, 317–328 (2005)

Yüksel, İ., Sandalcı, M., Çeribaşı, G., and Ö. Yüksek, 2011: Effects of global warming and climate change on water resources. *National 7th Coastal Engineering Symposium*, 21–23

Yuksel, U.D.: Examination of the air and surface temperatures in structural and green areas in the city: the case of Ankara. Ecology. **18**(69), 66–74 (2008)

Zareie, S., Khosravi, H., Nasiri, A.: Derivation of land surface temperature from Landsat thematic mapper (TM) sensor data and analyzing relation between land use changes and surface temperature. Solid Earth Discuss. 1–15 (2016a)

Zareie, S., Khosravi, H., Nasiri, A., Dastorani, M.: Using Landsat thematic mapper (TM) sensor to detect change in land surface temperature in relation to land use change in Yazd, Iran. Solid Earth. **7**, 1551–1564 (2016b)

Zhang, H., Qi, Z.F., Ye, X.Y., Cai, Y.B., Ma, W.C., Chen, M.N.: Analysis of land use/land cover change, population shift, and their effects on spatiotemporal patterns of urban heat islands in metropolitan Shanghai, China. Appl. Geogr. **44**, 121–133 (2013)

Zhang, F., Tiyip, T., Kung, H., Johnson, V.C., Maimaitiyiming, M., Zhou, M., Wang, J.: Dynamics of land surface temperature (LST) in response to land use and land cover (LULC) changes in the Weigan and Kuqa river oasis, Xinjiang, China. Arab. J. Geosci. **9**(7), 499 (2016)

Zhang, Y., Odeh, I.O.A., Han, C.: Bi-temporal characterization of land surface temperature in relation to impervious surface area, NDVI and NDBI, using a sub-pixel image analysis. Int. J. Appl. Earth Obs. Geoinf. **11**, 256–264 (2009)